Article

Multi-Level Wavelet Shannon Entropy-Based Method for Single-Sensor Fault Location

Qiaoning Yang * and Jianlin Wang

College of Information Science & Technology, Beijing University of Chemical Technology, 100029 Beijing, China; E-Mail: wangjl@mail.buct.edu.cn

* Author to whom correspondence should be addressed; E-Mail: yangqn@mail.buct.edu.cn; Tel.: +86-10-84830270.

Abstract: In actual application, sensors are prone to failure because of harsh environments, battery drain, and sensor aging. Sensor fault location is an important step for follow-up sensor fault detection. In this paper, two new multi-level wavelet Shannon entropies (multi-level wavelet time Shannon entropy and multi-level wavelet time-energy Shannon entropy) are defined. They take full advantage of sensor fault frequency distribution and energy distribution across multi-subband in wavelet domain. Based on the multi-level wavelet Shannon entropy, a method is proposed for single sensor fault location. The method firstly uses a criterion of maximum energy-to-Shannon entropy ratio to select the appropriate wavelet base for signal analysis. Then multi-level wavelet time Shannon entropy and multi-level wavelet time-energy Shannon entropy are used to locate the fault. The method is validated using practical chemical gas concentration data from a gas sensor array. Compared with wavelet time Shannon entropy and wavelet energy Shannon entropy, the experimental results demonstrate that the proposed method can achieve accurate location of a single sensor fault and has good anti-noise ability. The proposed method is feasible and effective for single-sensor fault location.

Keywords: fault location; wavelet transform; Shannon entropy; sensor fault

1. Introduction

Sensors have been widely employed for various monitoring and control applications to collect measurement of sensed events. Due to the possible harsh deployment environments, battery drain, and sensor aging, sensors are prone to failure. Measurement from a faulty sensor will lead to incorrect decisions and incorrect judgment. In practical applications, sensor fault identification and sensor fault location are two equally important issues. The former is to find whether there is any faults in sensor data, the latter is to determine which time data is reliable, which time data is not reliable. Fault location is the prerequisite for sensor replacement, maintenance, data deletion, and correction.

In the research field of sensor fault location, correlation analysis methods [1–5] and statistics methods [6–10] are commonly used. Wavelet transform, as a time-frequency analysis technique, has been widely used in many practical applications, such as feature extraction and noise elimination. Shannon entropy is a measure of the amount of information in the communication field. A new technique which associated wavelet transform with Shannon entropy was developed for signal analysis. Wang *et al.* [11] applied the wavelet time-entropy to extract features after wavelet packet decomposition, and the extracted features were used in a support vector machine method for identification of the normal and five types of abnormal heart sounds. He *et al.* [12] gave six different definitions about wavelet entropy, and used the wavelet entropy to identify fault in a power system. Chen *et al.* [13] discussed the difference between Shannon entropy and Tsallis entropy, and proposed wavelet packet Tsallis entropy to detect transient disturbances in power systems. Liu *et al.* [14] combined wavelet packet with Tsallis singular entropy to detect transient disturbances in power system. Bafroui *et al.* [15] extracted wavelet energy entropy and statistical metrics for the features of ball bearings, and used artificial neural network to diagnose faults of ball bearings.

In this paper, a methodology is proposed for single-sensor fault location. In the method, considering the characteristics of energy distribution and the characteristics of spectrum distribution across multi-subbands in the wavelet domain for sensor fault signals, multi-level wavelet time Shannon entropy and multi-level wavelet time-energy Shannon entropy are defined. The method firstly uses a criterion of maximum energy-to-Shannon entropy ratio to select the appropriate wavelet base for signal analysis, then applies two kinds of proposed multi-level wavelet Shannon entropy to locate sensor fault. This paper is organized as follows. In Section 2, several different sensor faults are introduced. Section 3 is the basic knowledge about discrete wavelet transform and wavelet Shannon entropy. In Section 4, the definition of two kinds of multi-level wavelet Shannon entropy and the proposed method are presented in detail. Using practical data, the performance of the proposed method is demonstrated in Section 5. Section 6 is the conclusion.

2. Sensor Fault

The sensor faults can be classified into various categories [16–18]. In this paper, we investigate five kinds of common sensor faults; that are bias, drift, stuck-at, complete failure, and precision degradation. They are introduced respectively as below.

Given the output of a sensor is $x(t)$:

$$x(t) = x'(t) + e_x \tag{1}$$

where $x(t)$ is the measured value of the sensed physical event, and $x'(t)$ is the true value of the sensed physical event, e_x is the error of the system.

2.1. Bias Fault

The measured values of sensor is bias from the true phenomenon by a constant amount. The data still exhibits normal patterns over an extended period. Based on Equation (1), the bias fault can be expressed as Equation (2):

$$e_x = C_0 u(t - t_0) \tag{2}$$

where C_0 is the constant for bias from the true value, t, represents the current moment, and t_0 represents the moment of bias occurrence.

2.2. Drift Fault

Sometimes, sensor performance may drift away from the original calibration formulas. That is, the drift parameters may change over time. Based on Equation (1), the drift fault can be expressed as Equation (3):

$$e_x = \alpha(t - t_0) \tag{3}$$

where α is a constant, representing the scale of drift, t represents the current moment, and t_0 represents the moment of drift occurrence.

2.3. Complete Failure

The sensor is fail suddenly, and the measured value of sensor is a constant amount. Complete failure is given as:

$$x(t) = \begin{cases} x'(t) & t \leq t_0 \\ C & t > t_0 \end{cases} \tag{4}$$

where C is a constant for the sensor's measured value, t, represents the current moment, and t_0 represents the moment of complete failure occurrence.

2.4. Stuck-at Fault

A "stuck-at" fault is defined as a series of data values that experiences zero or almost zero variation for a period of time. The zero variation must also be counter to the expected behavior of the phenomenon. The sensor may or may not return to normal operating behavior after the fault. It may follow either an unexpected jump or unexpected rate of change. The data around such a fault must exhibit some variation.

While it is similar to "complete failure", they differ in that the data value around the constant for stuck-at behave normally, and the data value is always be the same value after a complete failure occurrence. So complete failure is a special case of stuck-at failure.

2.5. Precision Degradation

The sensed capacity of the sensor goes poor, and the measurement precision degraded. Although it is difficult to find precision degradation, precision degradation have weakly impacts on system behavior. By contract, bias fault and drift fault is also not easy to be found, but they have big effect on system. Thus, the detection of bias, drift, and stuck-at faults are the main focus of this paper.

3. Discrete Wavelet Transform (DWT) and Wavelet Shannon Entropy

3.1. Discrete Wavelet Transform

Wavelet transform is a powerful tool to detect both stationary and transient signals. The wavelet transform technique has special benefits for describing signals at various localization levels in time, in addition to frequency domains [15,19]. Discrete wavelet transform is obtained by discretizing the scaling and shifting parameters in continuous wavelet transform. The discrete wavelet transform can be efficiently realized by means of a pair of low-pass and high-pass wavelet filters. These filters, also known as the quadrature mirror filters (QMF), are reconstructed from the selected wavelet and its corresponding scaling function. Through such a pair of filters, the signal is decomposed into low- and high-frequency components, respectively. The approximation coefficient represents the low-frequency component of the signal, and the detail coefficient corresponds to the high-frequency component. Usually, through the Mallat algorithm, a signal is decomposed and reconstructed in multi-scale. This procedure is expressed as follows:

$$\begin{cases} d_j(n) = \sum_k g(2n-k)a_{j-1}(k) \\ a_j(n) = \sum_k h(2n-k)a_{j-1}(k) \qquad j \geq 1 \\ a_0(n) = x(n) \end{cases} \tag{5}$$

where $x(n)$ is the analyzed original signal. $n = 1, 2, \ldots N$, N is the length of original signal. $h(n)$ and $g(n)$ denote low-pass filter and high-pass filter for decomposition, respectively. $d_j(n)$ and $a_j(n)$ denote the detail coefficient and the approximation coefficient in decomposition level j.

$$\begin{cases} D_j(n) = \sum_k G(2n-k)A_{j-1}(k) \\ A_j(n) = \sum_k H(2n-k)A_{j-1}(k) \qquad j \geq 1 \\ A_{j-1}(n) = A_j(n) + D_j(n) \end{cases} \tag{6}$$

where $H(n)$ and $G(n)$ denotes low-pass filter and high-pass filter for reconstruction, respectively. $D_j(n)$ and $A_j(n)$ denotes the reconstructed detail signal and the reconstructed approximation signal at each scale; that is, the single-branch reconstruction signal.

The frequency range corresponding to the decomposition coefficient at each level (or the single-branch reconstruction signal) was expressed as:

$$d_j(n) : \left[\frac{f_s}{2^{j+1}}, \frac{f_s}{2^j} \right] \qquad a_j(n) : \left[0, \frac{f_s}{2^{j+1}} \right] \tag{7}$$

where f_s is the sampling rate of signal. The original signal $x(n)$ can be expressed as:

$$x(n) = D_1(n) + A_1(n) = D_1(n) + D_2(n) + A_2(n) = \sum_{j=1}^{J} D_j(n) + A_J(n) \tag{8}$$

In order to unify expressions, $A_J(n)$ is denoted with $D_{J+1}(n)$. Thus, $x(n)$ can be expressed as Equation (9):

$$x(n) = \sum_{j=1}^{J+1} D_j(n) \tag{9}$$

In practical applications, wavelet transform combined with Shannon entropy is always used for signal processing. Here, two different wavelet Shannon entropies are introduced [12–13].

3.2. Wavelet Time Shannon Entropy (WTE)

A sliding-window W is defined at j-th single-branch reconstruction signal $\{D_j(n), n = 1, ..., N\}$, and the width of the window is $2 \leq w \leq N$. The sliding factor is $1 \leq \delta \leq w$. Then the sliding window should be expressed as:

$$\begin{aligned} W(m) &= \{D_j(n), n = 1 + m\delta, ..., w + m\delta\} \\ m &= 0, 1, 2, ..., M, M = (N - w) / \delta \end{aligned} \tag{10}$$

The sliding window is divided into the following R sections:

$$W(m) = \bigcup_{r=1}^{R} Z_r \tag{11}$$

where $\{Z_r = [s_{r-1}, s_r], r = 1, ...R\}$, $s_0 < s_1 < ... < s_R, s_0 = \min(W(m))$, $s_R = \max(W(m))$. Given $p_m(Z_r)$ as the probability that $D_j(n)$ falls into section Z_r, according to the classic probability theory, it is the proportion of the number of $D_j(n)$ within Z_r to the total number of coefficients in sliding window. Thus, the definition of wavelet time entropy at j scale is expressed as:

$$WTE_j(m) = -\sum_r p_m(Z_r) \log_a(p_m(Z_r)), m = 0, 1, 2, ..., M \tag{12}$$

3.3. Wavelet Energy Shannon Entropy (WEE)

Given the energy in sliding window W at j scale is $E_j(m)$.

$$E_j(m) = \sum_{n=1+m\delta}^{w+m\delta} (D_j(n))^2 \tag{13}$$

The definition of wavelet energy Shannon entropy is expressed as below.

$$WEE(m) = -\sum_j p_m(j) \log_a(p_m(j)), \quad m = 0, 1, 2, ..., M \tag{14}$$

where $E(m) = \sum_{j=1}^{J} E_j(m)$, and $p_m(j) = \dfrac{E_j(m)}{E(m)}$ is the total energy in W at all scale.

4. Methodology

4.1. Wavelet Selection Criterion [20–22]

In general, all the base wavelets can be used for implementing wavelet transform for signal analysis. For the faulty sensor signal under investigation, an appropriate wavelet, however, should be capable of extracting the sensor fault vibrations effectively. As it is known, the wavelet transform essentially measures the similarity between the signal to be analyzed and scaled version of a base wavelet. The more similar the analyzed signal to the wavelet base function is, the higher the magnitude of the wavelet decomposition coefficient. For a sensor fault signal, an appropriate wavelet will yield high magnitudes of wavelet coefficients. Meanwhile, the corresponding energy will be large, and the energy concentration will be high. In another word, an appropriate wavelet can extract the maximum amount of energy while minimizing the Shannon entropy of the corresponding wavelet coefficients. [20–22] combine the energy and Shannon entropy of a signal's wavelet coefficients and define an energy-to-Shannon Entropy ratio, denoted as (15), which is used to select an appropriate wavelet in this paper. The base wavelet that has produced the maximum energy-to-Shannon entropy ratio was chosen to be the most appropriate wavelet, *i.e.*, the maximum energy-to-Shannon entropy ratio criterion.

$$ratio(j) = \frac{E(j)}{S_{entropy}(j)} \tag{15}$$

where $E(j) = \sum_{k=1}^{K} |wt(j,k)|^2$ is the energy of wavelet coefficients at j scale, $wt(j,k)$ is the k-th wavelet coefficient of j scale, and K is the total number of wavelet coefficients.

$$S_{entropy}(j) = -\sum_{k=1}^{K} p_k \log_a p_k \tag{16}$$

where $a = 2$, the same as follows. p_k is the energy probability distribution of the wavelet coefficients, and $p_k = \frac{|wt(j,k)|^2}{E(j)}$. With $\sum_{k=1}^{K} p_k = 1$, and, if $p_k = 0$.

4.2. Proposed Multi-Level Wavelet Shannon Entropy

Through experimental analysis, we get the characteristics of the spectrum about faulty sensor data. The spectrum of faulty sensor data is concentrated in the low-frequency band primarily. Compared with the spectrum of normal sensor data, the spectrum of faulty sensor data differs not only in the low-frequency band but also in the high-frequency band. Thus, after applying wavelet transform to faulty sensor data, the feature of the sensor fault is reflected not only in the low-frequency sub-band but also in the high-frequency sub-band. The definition of wavelet time Shannon entropy in Equation (12) aims at the single sub-band, and cannot completely reflect the features of a sensor fault. In order to fully consider the feature of a sensor fault, single-branch reconstruction signals of all sub-bands are used to calculate the Shannon entropy.

When the selected wavelet base is applied to a faulty sensor signal, the magnitude of the wavelet coefficient in the fault-frequency sub-band is high, and other coefficients are low. In addition, the major

signal energy concentrates in this sub-band, *i.e.*, minimizing Shannon entropy in this sub-band [21]. Due to the fact that the energy can better represent the coefficient variation and coefficient distribution, the energy of a single-branch reconstruction signal of all sub-bands is used to calculate the Shannon entropy.

Considering all single-branch reconstruction signals and the corresponding energy as a whole, multi-level wavelet time Shannon entropy and multi-level wavelet time-energy Shannon entropy was proposed as a feature to locate a sensor fault. They are defined as follows.

4.2.1. Multi-Level Wavelet Time Shannon Entropy (MWTE)

A sliding window W is applied on single-brand reconstruction signal of all sub-band $\{D_j(n), j = 1, 2, \dots J+1, n = 1, \dots, N\}$, and all data in the sliding window is expressed as follows:

$$W_{J \times w}^D(m) = \begin{bmatrix} D_1(1+m\delta) & D_1(2+m\delta) & \dots & D_1(w+m\delta) \\ D_2(1+m\delta) & \ddots & & \vdots \\ \vdots & & \ddots & \vdots \\ \vdots & & & \vdots \\ D_{J+1}(1+m\delta) & \dots & \dots & D_{J+1}(w+m\delta) \end{bmatrix} \tag{17}$$

All data in $W_{J \times w}^D(m)$ are divided into R sections, $W_{J \times w}^D(m) = \bigcup_{r=1}^{R} Z_r^J$, therein $\{Z_r^J = [z_{r-1}^J, z_r^J], r = 1, \dots R\}$, $z_0^J < z_1^J < \dots < z_R^J$, $z_0^J = \min(W_{J \times w}^D(m)), z_R^J = \max(W_{J \times w}^D(m))$ and the multi-level wavelet time entropy is defined as:

$$MWTE(m) = -\sum_r p_m(Z_r^J) \log_a(p_m(Z_r^J)), m = 0, 1, 2, \dots, M \tag{18}$$

where $p_m(Z_r^J)$ is the probability that $D_j(n)$ falls into section Z_r^J, *i.e.*, the proportion of the number of $D_j(n)$ within Z_r^J to the total number of data in $W_{J \times w}^D(m)$, denoted as (19):

$$p_m(Z_r^J) = \frac{\#\{D_j(n) \in Z_r^J\}}{\#\{W_{J \times w}^D(m)\}} \tag{19}$$

4.2.2. Multi-level Wavelet Time-energy Shannon Entropy (MWTEE)

A sliding window W is applied to the energy of a single-band reconstruction signal in all sub-bands $\{(D_j(n))^2, j = 1, 2, \dots J+1, n = 1, \dots, N\}$, and all energy data in the sliding window is expressed as:

$$W_{J \times w}^E(m) = \begin{bmatrix} (D_1(1+m\delta))^2 & (D_1(2+m\delta))^2 & \dots & (D_1(w+m\delta))^2 \\ (D_2(1+m\delta))^2 & \ddots & & \vdots \\ \vdots & & \ddots & \vdots \\ \vdots & & & \vdots \\ (D_{J+1}(1+m\delta))^2 & \dots & \dots & (D_{J+1}(w+m\delta))^2 \end{bmatrix} \tag{20}$$

All data in $W_{J\times w}^{E}(m)$ are divided into R sections, $W_{J\times w}^{E}(m) = \bigcup_{r=1}^{R} E_{r}^{J}$, therein $\left\{ E_{r}^{J} = [e_{r-1}^{J}, e_{r}^{J}], r = 1, ...R \right\}$, $e_{0}^{J} < e_{1}^{J} < ... < e_{R}^{J}$, $e_{0}^{J} = \min(W_{J\times w}^{E}(m)), e_{R}^{J} = \max(W_{J\times w}^{E}(m))$. Then, the multi-level wavelet time-energy Shannon entropy is defined as:

$$MWTEE(m) = -\sum_{r} p_{m}(E_{r}^{J}) \log_{a}(p_{m}(E_{r}^{J})), m = 0, 1, 2, ..., M \tag{21}$$

where $p_{m}(E_{r}^{J})$ is the probability that $(D_{j}(n))^{2}$ falls into section E_{r}^{J}, *i.e.*, the proportion of the number of $(D_{j}(n))^{2}$ within E_{r}^{J} to the total number of energy-data in $W_{J\times w}^{E}(m)$, denoted as (22):

$$p_{m}(E_{r}^{J}) = \frac{\#\{(D_{j}(n))^{2} \in E_{r}^{J}\}}{\#\{W_{J\times w}^{E}(m)\}} \tag{22}$$

4.3. Multi-Level Wavelet Shannon Entropy Based Sensor Fault Localization Method

The following steps explain the proposed method in this paper. The corresponding flowchart is shown in Figure 1.
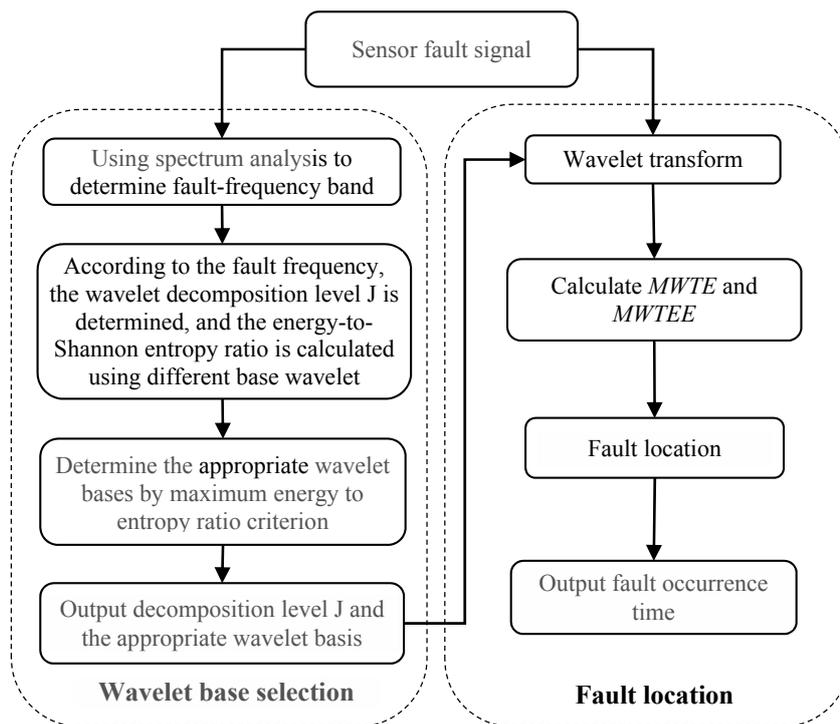

Figure 1. Flowchart of sensor fault location method.

(1) Base wavelet selection: using 20 kinds of base wavelets to calculate the energy-to-Shannon entropy of a fault sensor signal. According to the maximum energy-to-Shannon entropy criterion, the appropriate base wavelet is determined.

(2) Fault Location: calculate *MWTE* and *MWTEE* of the faulty signal, using their impulse peak position to locate the occurrence time of faults.

5. Experiments Result and Performance Analysis

In order to assess the feasibility and effectiveness of the proposed method, an actual sensor dataset is used in the following experiments.

The experimental dataset is comprised of time-series measurement recordings collected from an array of 72 metal-oxide gas sensor array-based chemical detection platform [23]. The sensor array includes nine portable modules, each with eight sensors. The data sampling rate is 100 Hz. One minute sampling data of one sensor is used as the original research object. Based on the original data, three kinds of faults (bias, stuck-at, and drift) are injected. For bias fault, the bias constant is 2% of the maximum of original data. In each stuck-at fault, there are two segments of data with constant value, 102% of the average value of the original data. In the drift fault groups, drift rate is 1% of the maximum original data per minute. Normal sensor data and fault sensor data are shown in Figure 2, respectively.
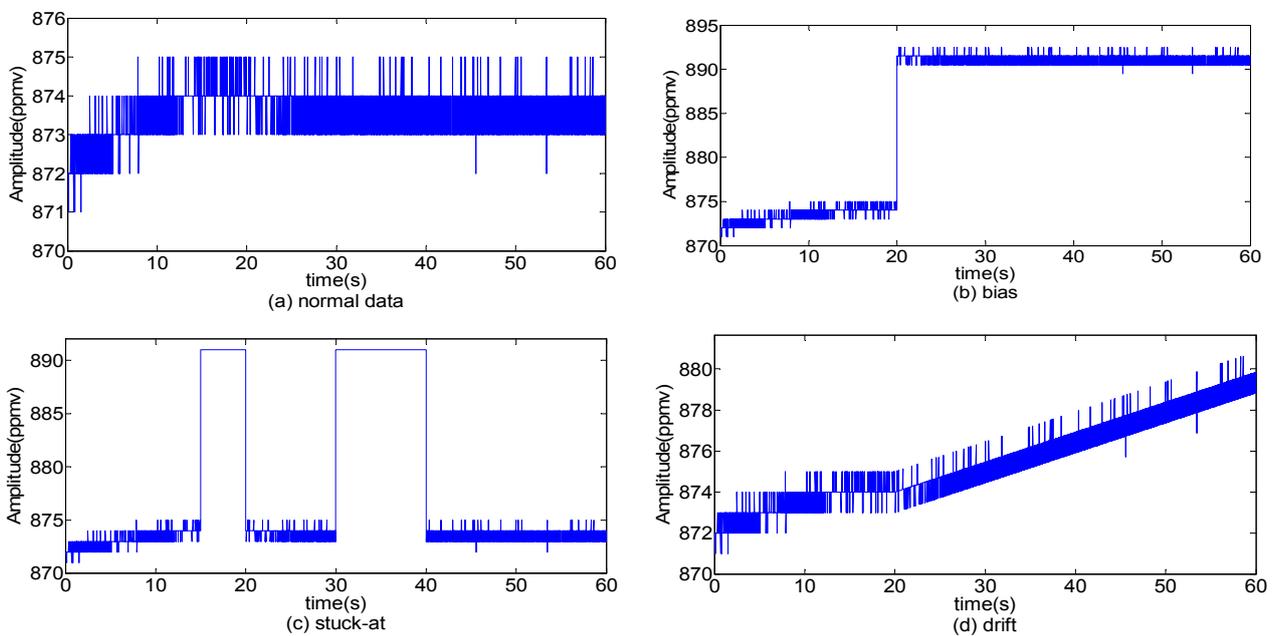

Figure 2. Normal sensor data and fault sensor data. (**a**) Normal data, (**b**) bias, (**c**) stuck-at, and (**d**) drift.

5.1. Wavelet Base Selection

Wavelet transform is applied to decompose signal, and each sub-band frequency range satisfies Equation (7). Given f_{id} is the frequency to be analyzed, the wavelet decomposition level J should satisfy Equation (23):

$$\frac{f_s}{2^{J+1}} \le f_{id} \le \frac{f_s}{2^J} \tag{23}$$

Under 100 Hz sampling rate, the original data is decomposed into J sub-bands using wavelet transform. The frequency range of each sub-band is shown in Table 1. From decomposition levels one to four, each sub-band has a different frequency range. Shown in Figure 3, all the different kinds of sensor fault signal spectrum mainly concentrate in the low frequency band, bandwidth is about 4 Hz.

Referring to Table 1, the fault is located in the 0 Hz–6.25 Hz frequency range, so the wavelet decomposition level *J* is chosen to be three.

Table 1. Frequency range for each decomposition level under a 100 Hz sampling rate.

Decomposition Level	Frequency Range (Hz)	Decomposition Level	Frequency Range (Hz)
L = 1	0–25	L = 3	0–6.25
L = 2	0–12.5	L = 4	0–3.125
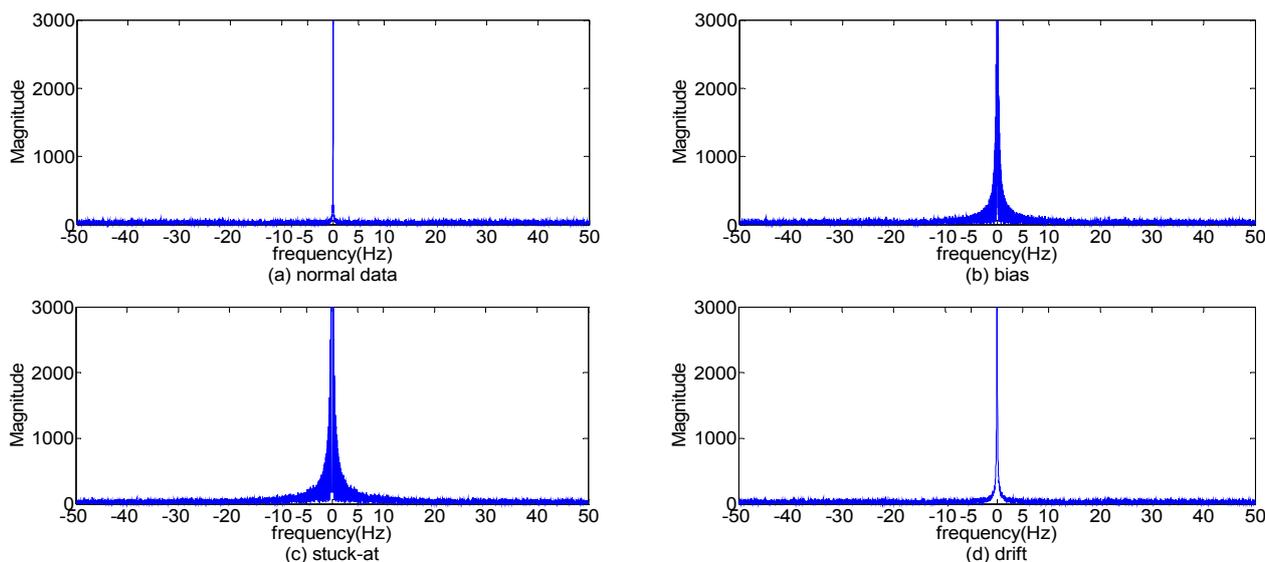
Figure 3. Magnitude spectrum of four signals. (**a**) Normal data, (**b**) bias, (**c**) stuck-at, and (**d**) Drift.

Table 2 shows the energy-to-Shannon entropy ratio after decomposition of sensor fault signals by using a different wavelet base. Before wavelet decomposition, the data is normalized. Based on the maximum energy-to-Shannon entropy ratio criterion, the Dmey wavelet possesses the highest values and, thus, is chosen as the most appropriate wavelet to process the sensor fault signal.

Table 2. Energy-to-Shannon entropy ratio of sensor faulty signal using different base.

Base Wavelet	Energy-to-Shannon Entropy Ratio	Base Wavelet	Energy-to-Shannon Entropy Ratio
Haar	888.3683	Coif2	897.3982
Db2	890.3625	Coif3	902.3987
Db4	894.3532	Coif4	908.4141
Db6	897.3165	Bior1.3	892.4105
Db8	901.3017	Bior2.4	895.4093
Sym1	888.3683	Bior2.6	899.4499
Sym2	890.3625	Dmey	976.5087
Sym3	892.3581	rBior1.3	892.4113
Sym4	894.4474	rBior2.4	895.4097
Coif1	892.3949	rBior2.6	899.4495

5.2. Fault Location and Performance Assessment

In this part, the fault location method proposed in this paper will be assessed, and the location performance of sensor fault will be compared with the location performance using the wavelet time Shannon entropy and wavelet energy Shannon entropy. Here, the window width $w = 20$, section numbers $R = 500$, sliding factor $\delta = 1$.

5.2.1. Experimental Result of the Proposed Method

Figures 4 and 5 are the positioning results of bias, drift, and stuck-at faults using MWTE and MWTEE separately.
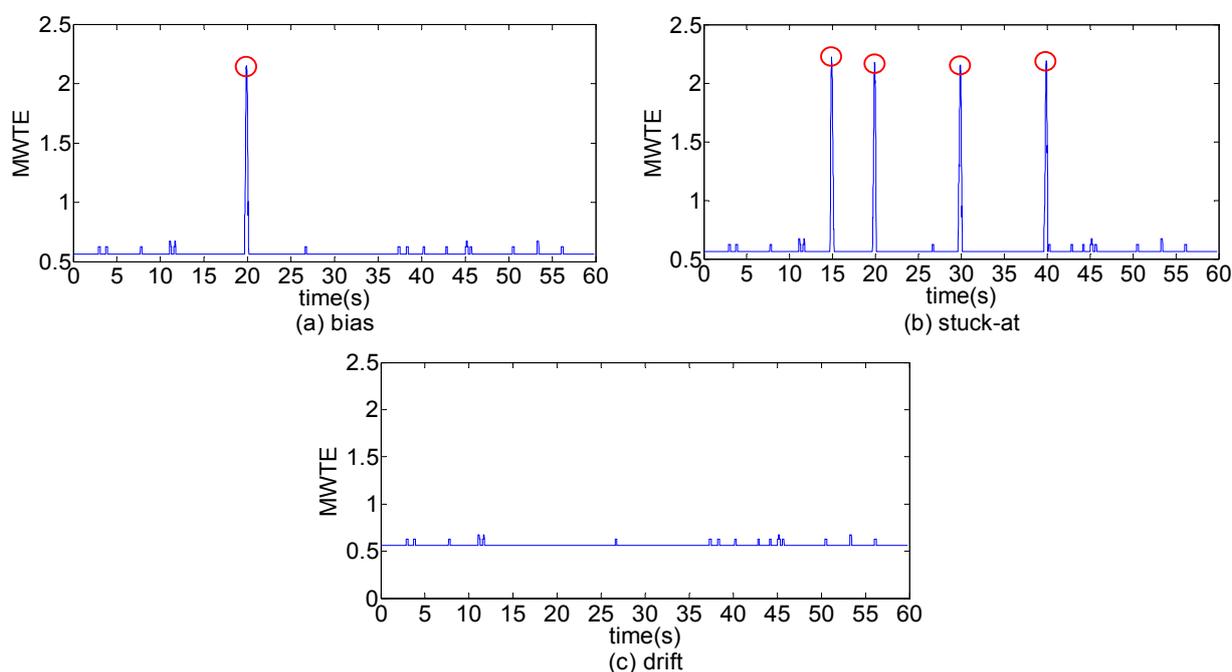
Figure 4. Multi-level wavelet time Shannon entropy (MWTE) of faults. (**a**) Bias, (**b**) stuck-at, and (**c**) drift.
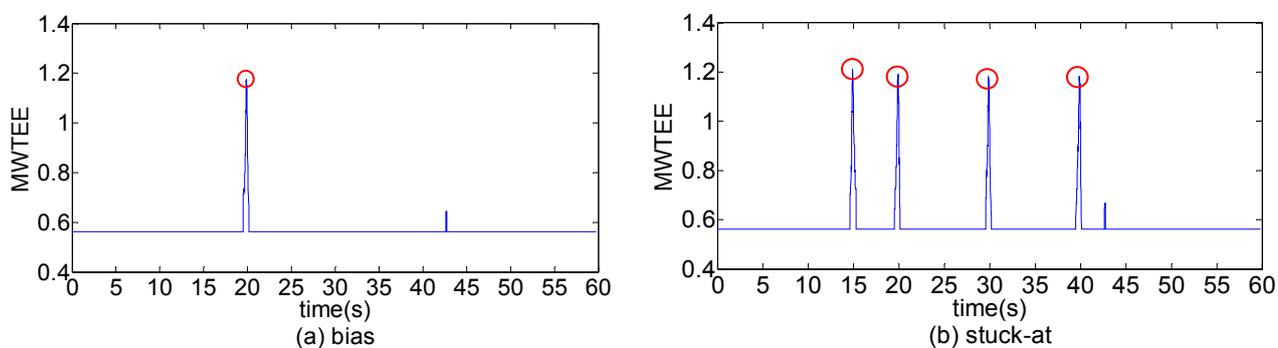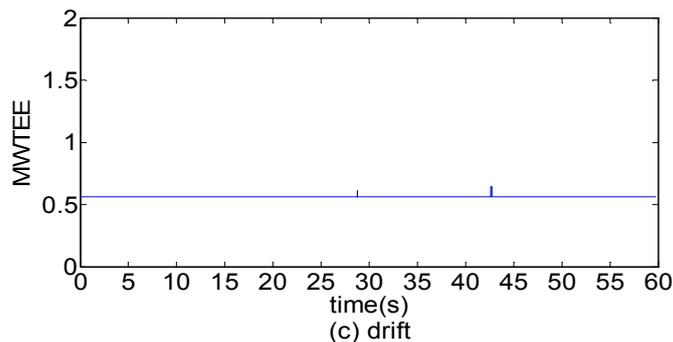

Figure 5. *Cont.*

Figure 5. Multi-level wavelet time-energy Shannon entropy (MWTEE) of faults. (**a**) Bias, (**b**) stuck-at, and (**c**) drift.

Compared with Figure 2, it is easy to find there is a significantly positive impulse at the time of 20 s in Figure 4a that is corresponding to the position of fault occurrence shown in Figure 2a. The same conclusion can be obtained that the stuck-at fault are located at the 15 s, 20 s, 30 s, and 40 s in Figure 4b. Compared Figure 4 with Figure 5, the position of impulse is occurred at the same time. Experiments show that MWTE and MWTEE can be used as a good mean to locate bias faults and stuck-at fault, but cannot be used to locate drift fault.

5.2.2. Experimental Result of Fault Location Using WTE and WEE

Figure 6 is the positioning results of bias, drift, and stuck-at fault using WTE. Compared with Figure 2, it is easy to find the wavelet time entropy, but cannot locate the occurrence time of bias and drift. For stuck-at faults, WTE can locate the occurrence time, but with low precision.
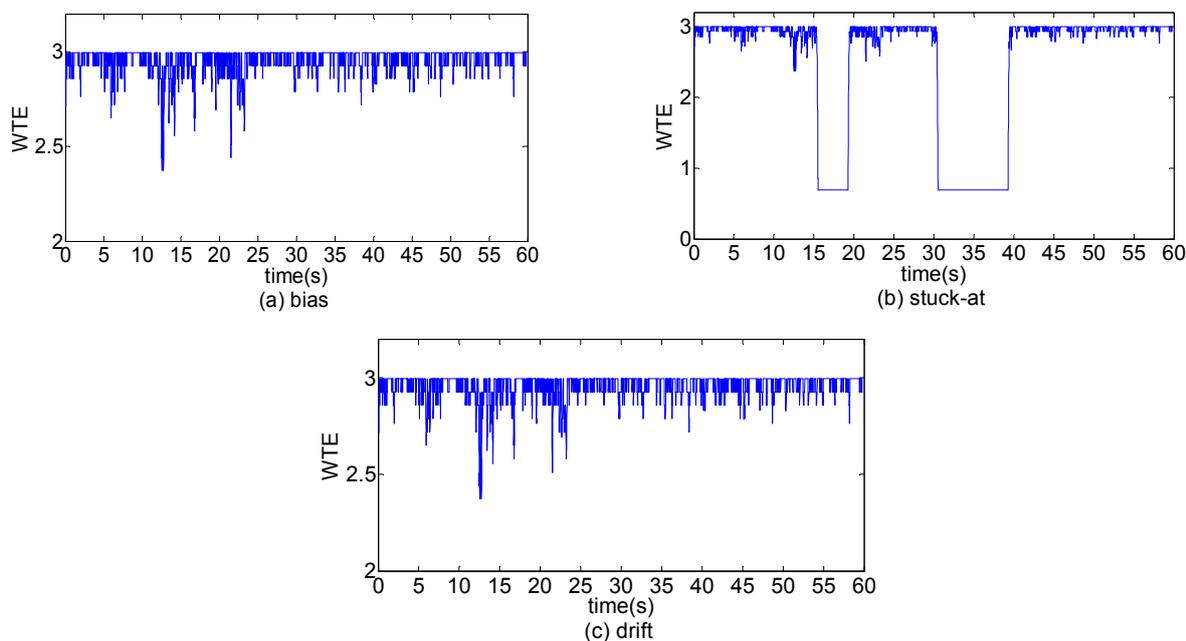

Figure 6. Wavelet Time Shannon Entropy (WTE) of faults. (**a**) Bias, (**b**) stuck-at, and (**c**) drift.
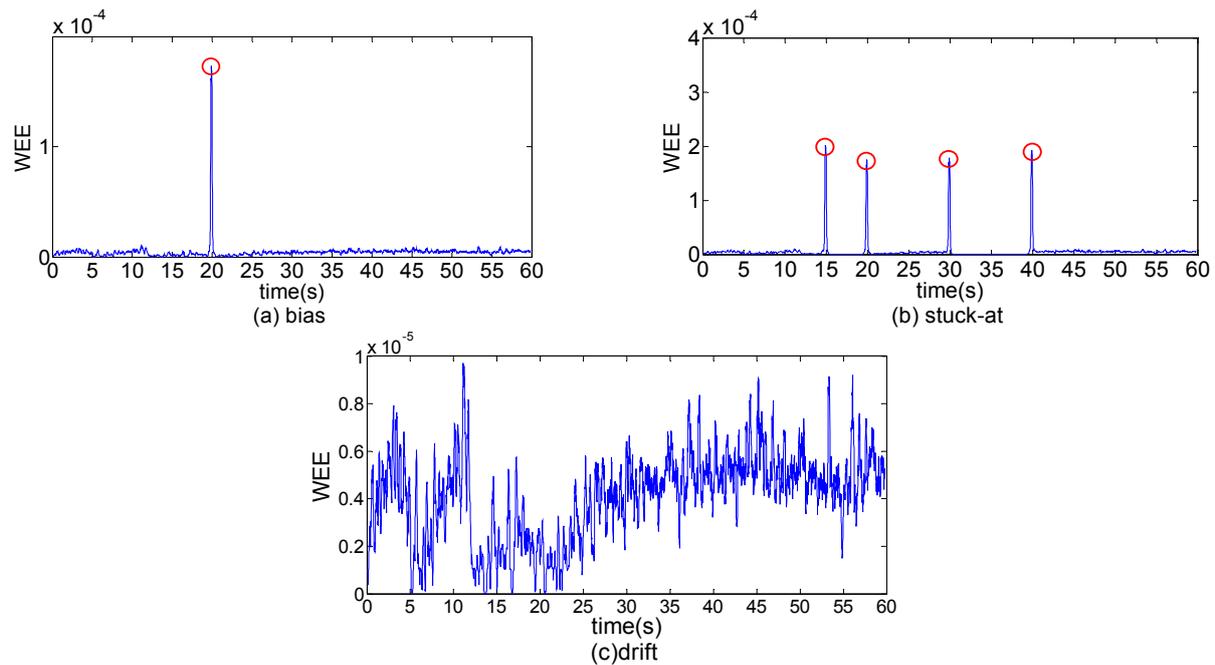
Figure 7. Wavelet Energy Shannon Entropy (WEE) of faults. (**a**) Bias, (**b**) stuck-at, and (**c**) drift.

Figure 7 shows the positioning results of bias, drift, and stuck-at fault using WEE. Compared with Figure 2, for bias and stuck-at faults, the position of the wavelet energy entropy's peak value is the same as the occurrence time of fault in Figure 2. That means WEE can be used to locate these two types of faults, but with low impulse amplitude of about 10^{-4}. Such small amplitude values are easy to be submerged in noise and are not suitable for practical applications. For drift fault, the WEE cannot locate the fault.

5.2.3. Fault Location Performance Analysis with Different Signal-Noise Ratio (SNR)

According to the above results, it can be concluded that in the absence of noise, the WEE, the proposed methods of this paper can locate the bias and suck-at faults. WTE only locates stuck-at faults.

In order to verify the location performance of the proposed method under noise, several different levels of Gaussian white noise are superimposed to the faulty signals, and location performance of WEE, WTE, MWTE, and MWTEE are examined. Figures 8–10 show the corresponding results of these four methods, when SNR = 45 db.

Compared to Figure 2, Figure 8 shows that WEE and WTE cannot locate the position of the fault under low noise. Instead, in Figures 9 and 10 the peak values of MWTE and MWTEE are consistent with the occurrence time of faults in Figure 2. Under the same conditions, MWTE and MWTEE can locate the faults. Additionally, MWTEE is more suitable for fault location than MWTE under low noise.
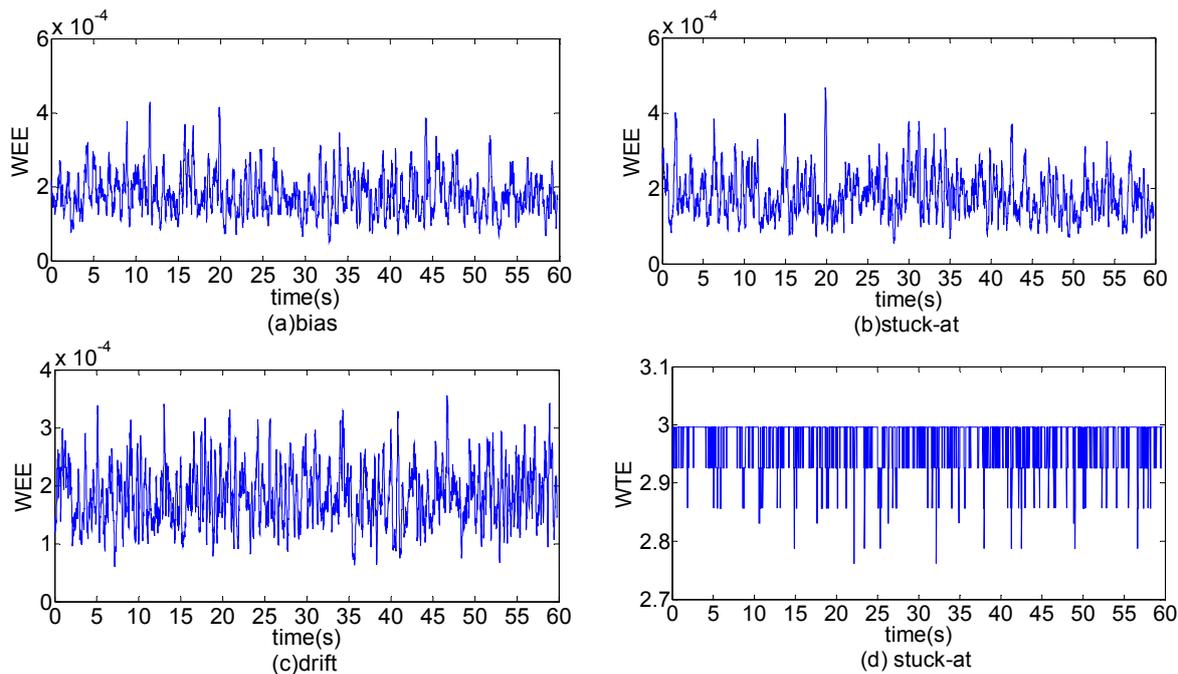
Figure 8. Wavelet Energy Shannon Entropy (WEE) of faults and Wavelet Time Shannon Entropy (WTE) of stuck-at fault when SNR = 45 dB. (**a**) Bias, (**b**) stuck-at, (**c**) drift, and (**d**) WTE of stuck-at.
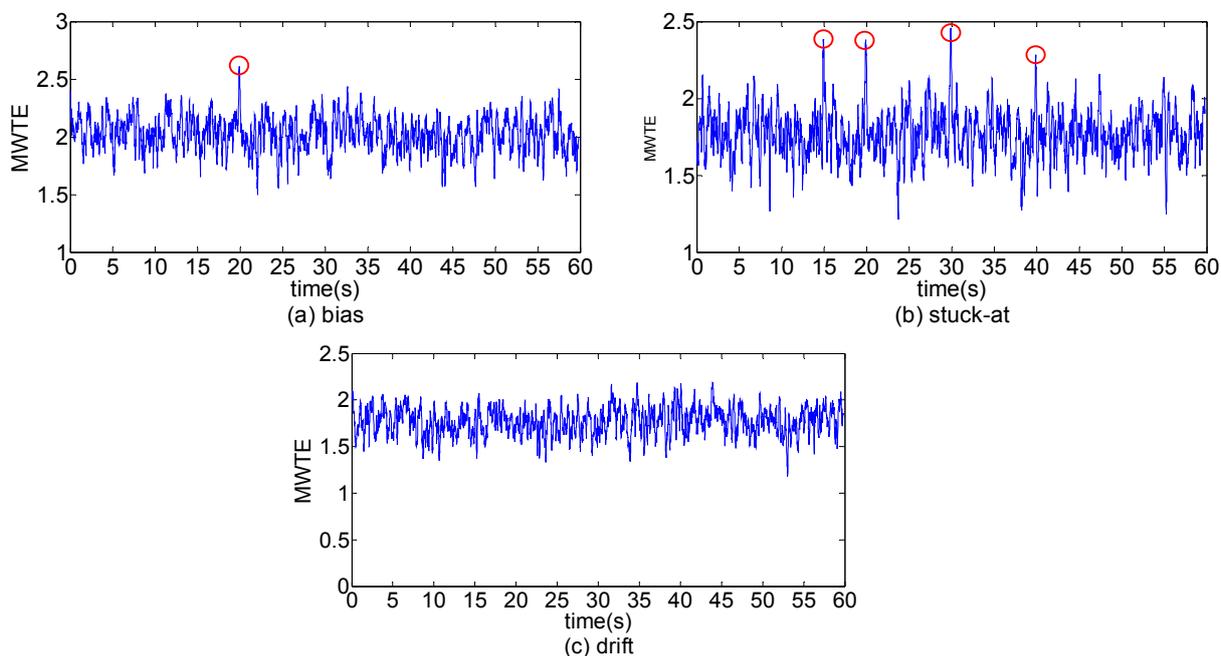

Figure 9. Multi-level wavelet time Shannon entropy (MWTE) of faults when SNR = 45 dB. (**a**) Bias, (**b**) stuck-at, and (**c**) drift.
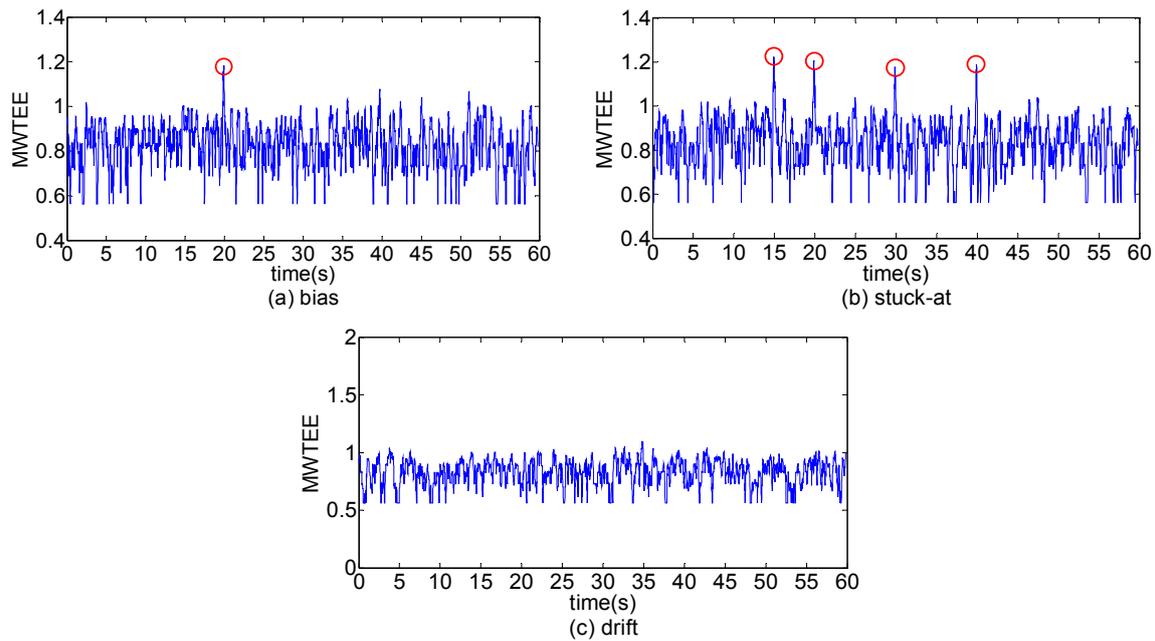
Figure 10. Multi-level wavelet time-energy Shannon entropy (MWTEE) of three type fault when SNR = 45 dB. (**a**) Bias, (**b**) stuck-at, and (**c**) drift.

6. Conclusion

Aiming at several typical single-sensor faults, bias, drift, and stuck-at, this paper proposed a new fault positioning method based on multi-level wavelet Shannon entropy. Considering fault signal frequency distribution characteristics, *i.e.*, sensor fault-frequency distributions across multi-subbands in wavelet domain, multi-level wavelet time Shannon entropy, and multi-level wavelet time-energy Shannon entropy are proposed to locate fault occurrence time.

The performance is evaluated using actual chemical gas concentration data. Experimental results demonstrate the proposed method in this paper is feasible and effective for bias and stuck-at fault locations. Compared with wavelet time entropy and wavelet energy entropy, the proposed method has good anti-noise performance. However, the method is not suitable for drift fault positioning. Follow-up studies will pay more attention on how to solve drift fault positioning.

Author Contributions

The work presented here was carried out in collaboration between all authors. Qiaoning Yang and Jianlin Wang designed the research and drafted the article. Qiaoning Yang performed the experiment, analyzed the data and revised the manuscript. Both authors have read and approved the final manuscript.

Conflicts of Interest

The authors declare no conflict of interest.

References

1. Lee, M.-H.; Choi,Y.-H. Fault detection of wireless sensor networks. *Comput. Commun.* **2008**, *31*, 3469–3475.

2. Zhuang, P.; Wang, D.; Shang, Y. Distributed distribution-based optimization for sensor fault detection. In Proceeding of 52nd IEEE International Midwest Symposium on Circuits and Systems, Cancun, Mexico, 2–5 August 2009; pp.280–283.

3. HajiBegloo, M.; Javadi, A. Fast fault detection in wireless sensor network. In Proceedings of Second International Conference on Digital Information and Communication Technology and it's Applications (DICTAP), Bangkok, Thailand, 16–18 May 2012; pp. 62–66.

4. Sarkis, M.; Hamdan, D.; EI Hassan, B. Aktouf, O.E. Online data fault detection in wireless sensor Networks. In Proceedings of 2nd International Conference on Advances in Computational Tools for Engineering Applications (ACTEA), Beirut, Lebanon, 12–15 December 2012; pp.61–65.

5. Lo, C.; Lynch, J.P.; Liu, M.Y. Distributed reference-free fault detection method for autonomous wireless sensor networks. *IEEE Sens. J.* **2013**, *13*, 2009–2019.

6. Chin, G.; Choudhury, S.; Kangas, L.; McFarlane, S.; Marquez, A. Fault detection in distributed climate sensor networks using dynamic bayesian networks. In Proceedings of Sixth IEEE International Conference on e–Science, Brisbane, Australia, 7–10 December 2010; pp. 121–128.

7. Zhang, Y.; Bingham, C.; Gallimore, M.; Yang, Z.J.; Stewart, J. Fault detection and diagnosis based on Y-indices and residual errors. In Proceedings of 15th International Symposium Conference on MECHATRONIKA, Prague, Czekh, 5–7 December 2012.

8. Korkali, M.; Abur, A. Detection, identification, and correction of bad sensor measurements for fault location. In Proceedings of IEEE Conference on Power and Energy Society General Meeting, San Diego, CA, USA, 22–26 July 2012.

9. De Paola, A.; Lo Re, G.; Milazzo, F.; Ortolani, M. QoS-Aware fault detection in wireless sensor networks. *Int. J. Distrib. Sens. Netw.* **2013**, *2013*, doi:10.1155/2013/165732.

10. Xie, Y.X.; Chen, X.G.; Zhao, J. Adaptive and online fault detection using RPCA algorithm in wireless sensor network nodes. In Proceedings of Second International Conference on Intelligent Systems Design and Engineering Application, Sanya, China, 6–7 January 2012; pp. 1371–1374.

11. Wang, Y.; Li, W.Z.; Zhou, J.L.; Li, X.H.; Pu, Y.F. Identification of the normal and abnormal heart sounds using wavelet-time entropy features based on OMS-WPD. *Futur. Gener. Comput. Syst.* **2014**, *37*, 488–495.

12. He, Z.Y.; Chen, X.Q.; Luo, G.M. Wavelet Entropy measure definition and its application for transmission line fault detection and identification; (Part I: Definition and methodology). In Proceedings of International Conference on Power System Technology, Chongqing, China, 22–26 October 2006.

13. Chen, J.K. Research on Feature Extraction and Recognition of Transient Signals in Power System Based on Wavelet Entropy. Doctoral Thesis, Harbin Institute of Technology, Harbin, China, June 2011.

14. Liu, Z.G.; Hu, Q.L.; Cui, Y.; Zhang, Q.G. A new detection approach of transient disturbances combining wavelet packet and Tsallis entropy. *Neurocomputing* **2014**, *142*, 393–407.

15. Bafroui, H.H.; Ohadi, A. Application of wavelet energy and Shannon entropy for feature extraction in gearbox fault detection under varying speed conditions. *Neurocomputing* **2014**, *133*, 437–445.

16. Chen, Y.; Lan, L. Fault detection, diagnosis and data recovery for a real building heating/cooling billing system. *Energy Convers. Manag.* **2010**, *51*, 1015–1024.

17. Liu, H.B.; Huang, M.Z.; Janghorban, I.; Ghorbannezhad, P.; ChangKyoo, Y. Faulty sensor detection, identification and reconstruction of indoor air quality measurements in a subway station. In Proceedings of 11th International Conference on Control, Automation and Systems, Gyeonggi-do, Korea, 26–29 October 2011; pp. 323–328.

18. Ni, K.; Ramanathan, N.; Chehade, M.N.H.; Balzano, L.; Nair, S.; Zahedi, S.; Kohler, E.; Pottie, G.; Hanse, M.; Srivastava, M. Sensor network data fault types. *ACM Trans. Sens. Netw.* **2009**, *5*, doi:10.1145/1525856.1525863.

19. Wu, J.D.; Chen, J.C. Continuous wavelet transform technique for fault signal diagnosis of internal combustion engines. *NDT & E Int.* **2006**, *39*, 304–311.

20. Kankar, P.K.; Sharma, S.C.; Harsha, S.P. Fault diagnosis of ball bearings using continuous wavelet transform. *Appl. Soft Comput.* **2011**, *11*, 2300–2312.

21. Yan, R.Q.; Gao, R.X. Base Wavelet selection for bearing vibration signal analysis. *Int. J. Wavel. Multi-Resolut. Inf. Process* **2009**, *7*, 411–426.

22. Yan, R.Q. Base Wavelet Selection Criteria for Non-Stationary Vibration Analysis in Bearing Health Diagnosis. Doctoral Thesis, University of Massachusetts Amherst, United States, May 2007.

23. Gas sensor arrays in open sampling settings Data Set. Available online: http://archive.ics.uci.edu/ml/datasets/Gas+sensor+arrays+in+open+sampling+settings (accessed on 14 October 2015).